






## IN SILICO INVESTIGATIONS OF TRIAZOLE-TRIMETHOXYPHENYL DERIVATIVES AS ANTI-PROLIFERATIVE AGENTS AGAINST ADENOCARCINOMIC HUMAN ALVEOLAR BASAL EPITHELIAL CELLS (A549): DFT, QSAR AND MOLECULAR DOCKING APPROACHES

Ameh Ojima Sunday<sup>a,\*</sup>, Shehu Abdullahi<sup>b,\*</sup>, Obiyenwa Kehinde Gabriel<sup>c,\*</sup>, Osang Moses<sup>d,\*</sup>,  
Semire Banjo<sup>e,\*†</sup>

<sup>a</sup>Department of Chemistry, Federal University Lokoja, Kogi State, Nigeria

<sup>†</sup>Computational Chemistry Laboratory, Department of Pure and Applied Chemistry, Ladoke Akintola, University of Technology, P.M.B. 4000, Ogbomoso, Oyo-State, Nigeria.

- |   |   |
|---|---|
| a) ✉ <a href="mailto:amehojimasunday@gmail.com">amehojimasunday@gmail.com</a>               |  <a href="https://orcid.org/0009-0008-8901-1692">https://orcid.org/0009-0008-8901-1692</a> |
| b) ✉ <a href="mailto:abdullahi.shehu@fulokoja.edu.ng">abdullahi.shehu@fulokoja.edu.ng</a>   |  <a href="https://orcid.org/0000-0002-7751-2392">https://orcid.org/0000-0002-7751-2392</a> |
| c) ✉ <a href="mailto:gabriel.obiyenwa@fulokoja.edu.ng">gabriel.obiyenwa@fulokoja.edu.ng</a> |  <a href="https://orcid.org/0000-0003-0184-8807">https://orcid.org/0000-0003-0184-8807</a> |
| d) ✉ <a href="mailto:osangmoses3@gmail.com">osangmoses3@gmail.com</a>                       |  <a href="https://orcid.org/0009-0000-5487-2603">https://orcid.org/0009-0000-5487-2603</a> |
| e) ✉ <a href="mailto:bsemire@lautech.edu.ng">bsemire@lautech.edu.ng</a>                     |  <a href="https://orcid.org/0000-0002-4173-9165">https://orcid.org/0000-0002-4173-9165</a> |

Twenty-eight sets of synthesized triazole-trimethoxyphenyl derivatives (TPDs) were considered as anti-proliferative drugs against human alveolar basal epithelial (A549) cancer cell lines using DFT, QSAR, ADMET profile and molecular docking methods. The considered compounds were used to develop a robust QSAR model, which was used to design new TPD compounds that could serve as anti-proliferative drug candidate against human alveolar basal epithelial (A549) cancer. The parameters obtained from DFT calculations such as the HOMO, LUMO, Dipole moment, chemical hardness and softness favoured TPD-11 and TPD-25 over etoposide as strong inhibitors against human alveolar basal epithelial cancer cell (A549), which agreed with the experimental data. The QSAR modeling and validation indicated the major influence of Moran autocorrelation – lag 4/weighted by polarizabilities (MATS4p), Centered Broto-Moreau autocorrelation - lag 7/weighted by charges (ATSC7c), Minimum E-State descriptors of strength for potential Hydrogen Bonds of path length 3 (minHBint3) and Count of atom-type E-State: C (naasC) descriptors on the reported anticancer activity of the drugs in the A549- MLR-GFA QSAR ( $R^2 = 0.8146$ , adjusted  $R^2 = 0.7874$ ,  $Q^2_{\text{Loo}} = 0.6015$  and  $R^2 - Q^2_{\text{Loo}} = 0.2582$ ). Using the model data, four new TPDs (NTPD-3, NTPD-4, NTPD-6 and NTPD-9) were proposed. The DFT and molecular docking analysis showed that these four compounds could be good inhibitors against A549 than etoposide. However, the ADMET (absorption, distribution, metabolism, excretion, and toxicity) properties revealed NTPD-6 showed excellent pharmacokinetic and toxicological profiles and might serve as a road map for new and more effective anticancer agents.

**Keywords:** Triazole–Trimethoxyphenyl, anti-cancer, DFT, QSAR, molecular docking.

### Introduction

High morbidity and mortality from both communicable and non-communicable diseases still have a negative influence on humanity. Non-communicable diseases (NCDs) have a significant financial burden on population in addition to causing sickness and mortality [1]. NCDs include chronic lung disease, cancer, diabetes, heart disease, and stroke which account for over 70% of all fatalities globally; heart disease and cancer have been described as leading cause of death among NCDs [2]. It had been estimated that over 10.3 million people died of cancer in 2020 with 2.26 million died of breast cancer new cases, lung cancer (2.21 million), colon and rectum cancer (1.93 million), prostate cancer (1.41 million), skin cancer (1.20 million) and stomach cancer (1.09 million); and with about 19.3 million new cases of cancer disease predicted [2,3]. Muka et al., (2015) [4] noted that NCDs place a heavy financial strain on healthcare budgets and thus on national welfare which may only get worse over time, if drastic measures are not taken. Therefore, cancer compared to the other NCDs call for special attention and consideration [5].

Recent developments in anticancer medications have considerably improved quality of life of cancer patients and have increase the rate of cancer survival. However, a favorable initial response to treatment changes afterwards, thereby leading to cancer relapse and recurrence [6]. Consequently, there is continuous research for new substances that can effectively act against this disease with little

© Sunday, A. O., Abdullahi, S., Gabriel, O. K., Moses, O., Banjo, S., 2025

 This is an open access article distributed under the terms of the Creative Commons Attribution License 4.0.

or no side effect. In drug development, researchers focus on the organic and biochemical reactions of drug substances with their targets as well as the synthesis and analysis of drug substances [7]. Therefore, there has been an increasing interest by researchers all over the world in exploring all available options; evaluating potential anticancer agents with the hope of discovering effective drugs for cancer. Also, several ongoing efforts are being made by the medical community aimed at identifying novel anticancer targets [8].

Among a class of nitrogen-containing heterocyclic compounds with interesting structures for medicinal properties is triazole derivatives due to their important chemical and biological properties that are stable against metabolic degradations and show target selectivity as well as several pharmacological activities [9 - 13]. Triazole functions well as a linker to connect different pharmacophores, thus, hybrid substances containing triazole have demonstrated the ability to decrease tumor growth, invasion, and metastasis by altering various signaling pathways. This is made possible by its capacity to form a variety of non-covalent interactions with various biological targets, including hydrogen bonds, van der Waals forces, hydrophobic interactions, and dipole-dipole bonds. This is what gives the compound its wide range of therapeutic properties, including its antibacterial [14], anti-malarial [15], antifungal [16]), antiviral [17], antitubercular [18], and anticancer activities [19, 20].

However, it has been observed that the high prevalence of resistance makes employing single chemicals as anticancer medicines in targeting protein or enzyme ineffective in treating cancer cells [21]. Therefore, several hybrids of triazole compounds have been synthesized and evaluated for their anticancer activities, such as triazole-benzimidazole-chalcone [22], triazole-quinazoline [23], Indole-Thiazolidinedione-Triazole [24], Coumarin-triazole [25], Quinolone-Triazole [26], triazolo[4,5-d]pyrimidine [27, 28], Triazole-Pyrimidine-Urea [29, 30].

According to reports [31, 32], trimethoxyphenyl compounds have also been shown to operate as a pharmacophoric group that enhances the anticancer activities of various natural anticancer drugs, including colchicine, combretastatin, podophyllotoxin, and poly-methoxychalcone. The trimethoxyphenyl-based compounds might be a viable way to get around some of the issues with the current anticancer medications that have been described. 5-amino-1,2,4-triazoles based on trimethoxyphenyl have been identified as promising antimitotic possibilities against CEM and Hela cells [33]. Also, a series of 3-(benzylthio)-4H-1,2,4-triazoles bearing trimethoxyphenyl scaffold were synthesized and tested against different cancer cell lines; the results revealed that 4-[3-[(4-methoxyphenyl)methylsulfanyl]-5-(3,4,5-trimethoxyphenyl)-1,2,4-triazol-4-yl]-N,N-dimethylaniline was a promising against colon cancer (HCT116 cell line) [33]. Furthermore, triazolothiadiazine, 4-amino-5-aryl-4H-1,2,4-triazoles and triazolothiadiazine with trimethoxy substituent were evaluated against cancer cells and the results were promising [34]. Recently, triazoles-trimethoxyphenyl hybrids were synthesized and evaluated using both experimental and in silico methods against cancer cells (A549, MCF7, and SKOV3) with etoposide as standard drug. The results revealed that most of the compounds inhibitory activities were comparable to that of the standard with some compounds having outstanding inhibitory properties [35].

Therefore, in this work, in silico methods would be used to further evaluate triazole - trimethoxyphenyl hybrids reported by Ansari et al., [35] as displayed in Figure 1 and Table 1. Although molecular docking of these compounds has been carried out, this study would lay emphasis on the development of robust QSAR using multiple linear regression-Genetic Algorithm (MLR-GA) to propose new set of triazole-trimethoxyphenyl hybrids with enhanced anticancer activity against adenocarcinomic human alveolar basal epithelial cells (A549). Thus, the aim of this work is to develop robust QSAR model, designed novel triazole-trimethoxyphenyl hybrids, predict their inhibitory properties, molecular docking analysis and ADMET profiling of the novel triazole - trimethoxyphenyl derivatives.

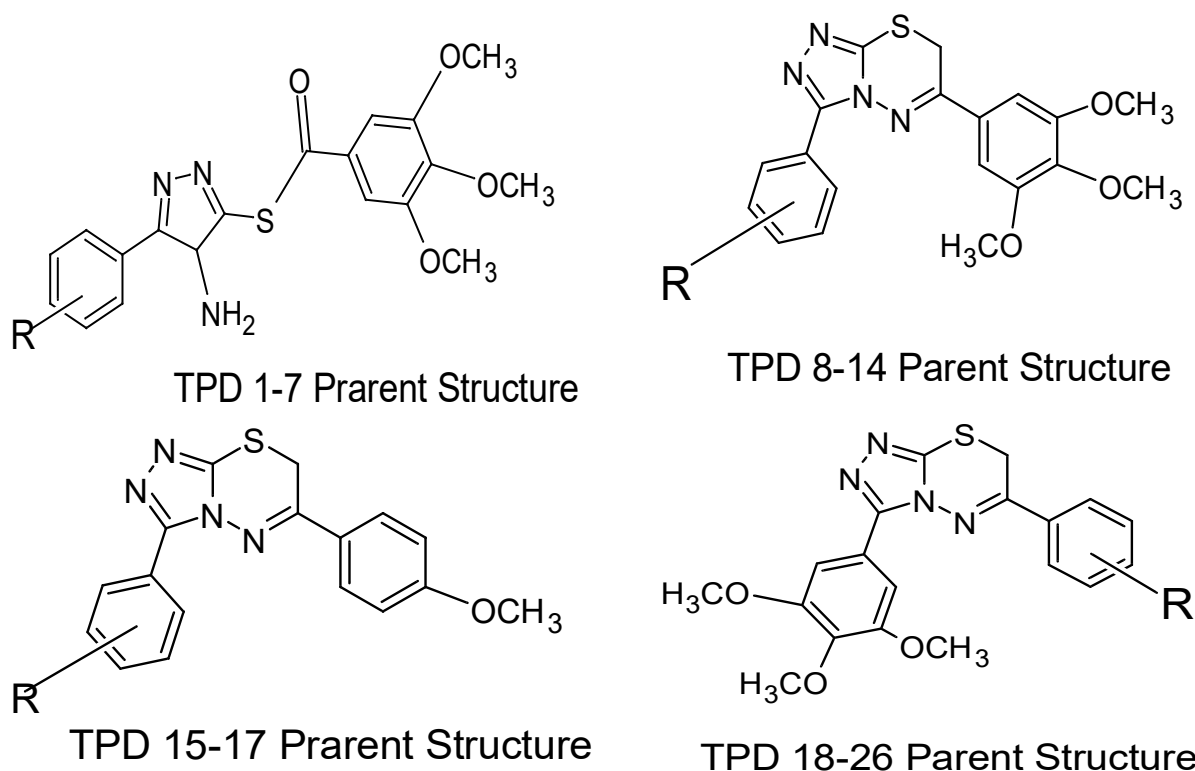


Figure 1: The schematic structures of the studied molecules triazole -trimethoxyphenyl hybrids [35]

Table 1. Structures, IUPAC names and observed  $IC_{50}$  of the triazole -trimethoxyphenyl hybrids used in training and test sets against adenocarcinomic human alveolar basal epithelial cells (A549).

Mole- cule	R	IUPAC Name	$IC_{50}$ $\mu$ M (A549)
TPD 1	H	2-[(4-amino-5-phenyl-1,2,4-triazolidin-3-yl)sulfanyl]-1-(3,4,5-trimethoxyphenyl)ethanol	3.95
TPD 2	4-CH <sub>3</sub>	2-[[4-amino-5-(4-methylphenyl)-1,2,4-triazol-3-yl]sulfanyl]-1-(3,4,5-trimethoxyphenyl) ethanone	4.39
TPD 3	4-OH	2-[[4-amino-5-(4-hydroxyphenyl)-1,2,4-triazol-3-yl]sulfanyl]-1-(3,4,5-trimethoxyphenyl)eth2-[[4-amino-5-(4-chlorophenyl)-1,2,4-triazol-3-yl]sulfanyl]-1-(3,4,5-trimethoxyphenyl)ethanone	4.20
TPD 4	3-Br	2-[[4-amino-5-(3-bromophenyl)-3,5-dihydro-1,2,4-triazol-3-yl]sulfanyl]-1-(3,4,5-trimethoxyphenyl)ethanol, 2-[[4-amino-3-(3-bromophenyl)-3,5-dihydro-1,2,4-triazol-5-yl]sulfanyl]-1-(3,4,5-trimethoxyphenyl)ethanol	3.67
TPD 5	4-OCH <sub>3</sub>	2-[[4-amino-5-(4-methoxyphenyl)-1,2,4-triazol-3-yl]sulfanyl]-1-(3,4,5-trimethoxyphenyl)ethanone	2.58
TPD 6	4-Cl	2-[[4-amino-5-(4-chlorophenyl)-1,2,4-triazol-3-yl]sulfanyl]-1-(3,4,5-trimethoxyphenyl) ethanone	2.81
TPD 7	2,4-Cl <sub>2</sub>	2-[[4-amino-5-(2,4-dichlorophenyl)-1,2,4-triazol-3-yl]sul-fanyl]-1-(3,4,5-trimethoxyphenyl)ethanone	3.79
TPD 8	H	3-phenyl-6-(3,4,5-trimethoxyphenyl)-7H-[1,2,4]triazolo[3,4-b][1,3,4]thiadiazine	3.71
TPD 9	4-CH <sub>3</sub>	3-(4-methylphenyl)-6-(3,4,5-trimethoxyphenyl)-7H-[1,2,4]triazolo[3,4-b][1,3,4]thiadiazine	4.57
TPD 10	4-OH	4-[6-(3,4,5-trimethoxyphenyl)-7H-[1,2,4]triazolo[3,4-b][1,3,4]thiadiazin-3-yl]phenol	4.17

TPD 11	3-Br	3-(3-bromophenyl)-6-(3,4,5-trimethoxyphenyl)-7H-[1,2,4]triazolo[3,4-b][1,3,4]thiadiazine	0.67
TPD 12	4-OCH <sub>3</sub>	3-(4-methoxyphenyl)-6-(3,4,5-trimethoxyphenyl)-7H-[1,2,4]triazolo[3,4-b][1,3,4]thiadiazine	3.20
TPD 13	4-Cl	3-(4-chlorophenyl)-6-(3,4,5-trimethoxyphenyl)-7H-[1,2,4]triazolo[3,4-b][1,3,4]thiadiazine	3.94
TPD 14	2,4-Cl <sub>2</sub>	3-(2,4-dichlorophenyl)-6-(3,4,5-trimethoxyphenyl)-7H-[1,2,4]triazolo[3,4-b][1,3,4]thiadiazine	2.73
TPD 15	H	6-phenyl-3-(3,4,5-trimethoxyphenyl)-7H-[1,2,4]triazolo[3,4-b][1,3,4]thiadiazine	1.04
TPD 16	4-OCH <sub>3</sub>	6-(4-methoxyphenyl)-3-(3,4,5-trimethoxyphenyl)-7H-[1,2,4]triazolo[3,4-b][1,3,4]thiadiazine	3.60
TPD 17	3,4-(CH <sub>3</sub> ) <sub>2</sub>	6-phenyl-3-(3,4,5-trimethoxyphenyl)-7H-[1,2,4]triazolo[3,4-b][1,3,4]thiadiazine	2.50
TPD 18	3,4,5-(CH <sub>3</sub> ) <sub>3</sub>	3,6-bis(3,4,5-trimethoxyphenyl)-7H-[1,2,4]triazolo[3,4-b][1,3,4]thiadiazine	4.00
TPD 19	4-F	6-(4-fluorophenyl)-3-(3,4,5-trimethoxyphenyl)-7H-[1,2,4]triazolo[3,4-b][1,3,4]thiadiazine	2.80
TPD 20	2,4-F <sub>2</sub>	6-(2,4-difluorophenyl)-3-(3,4,5-trimethoxyphenyl)-7H-[1,2,4]triazolo[3,4-b][1,3,4]thiadiazine	2.15
TPD 21	4-Cl	6-(4-chlorophenyl)-3-(3,4,5-trimethoxyphenyl)-7H-[1,2,4]triazolo[3,4-b][1,3,4]thiadiazine	4.97
TPD 22	4-Br	6-(4-bromophenyl)-3-(3,4,5-trimethoxyphenyl)-7H-[1,2,4]triazolo[3,4-b][1,3,4]thiadiazine	3.15
TPD 23	4-OH	4-[3-(3,4,5-trimethoxyphenyl)-7H-[1,2,4]triazolo[3,4-b][1,3,4]thiadiazin-6-yl]phenol	5.01
TPD 24	3,4-(OH) <sub>2</sub>	4-[3-(3,4,5-trimethoxyphenyl)-7H-[1,2,4]triazolo[3,4-b][1,3,4]thiadiazin-6-yl]phenol	3.23
TPD 25	4-CH <sub>3</sub>	6-(4-methylphenyl)-3-(3,4,5-trimethoxyphenyl)-7H-[1,2,4]triazolo[3,4-b][1,3,4]thiadiazine	0.60
TPD 26	4-Ph	6-(4-phenylphenyl)-3-(3,4,5-trimethoxyphenyl)-7H-[1,2,4]triazolo[3,4-b][1,3,4]thiadiazine	4.01
Standard		Etoposide	2.99

### In silico Methods

A data set of twenty-six triazole-trimethoxyphenyl hybrids and their anti-cancer activities were obtained from the work of Ansari et al (2019) as shown in Figure 1 and Table 1. The biological activities of the ligands were expressed as half-maximum inhibitory concentration ( $IC_{50}$ ). The  $IC_{50}$  values were subjected to data transformation by taking the negative logarithm to the base of 10 according to the formula:

$$pIC_{50} = -\log(IC_{50}) \times 10^{-6} \quad (1)$$

These compounds were optimised at DFT-B3LYP/6-31G(d,p) methods for molecular geometries using Spartan 14 software as described by [36, 37]. The frequency calculations were carried out on the optimised structure to ascertain minima equilibrium characterized by positive harmonic frequencies [38, 39]. The molecular parameters estimated from the ground state optimized structures were the frontier orbital energies (the HOMO, LUMO and energy gap), chemical hardness ( $\eta = (E_{LUMO} - E_{HOMO})/2$ ) chemical potential ( $\mu = (E_{LUMO} + E_{HOMO})/2$ ), electrophilicity index ( $\omega = \frac{\mu^2}{2\eta}$ ) and dipole moment [40, 41].

### QSAR modelling

The optimized structures were converted to \*.sdf format for generation of molecular descriptors using Padel-Descriptor software version 2.21 (Rivera-Delgado et al., 2019). Over 1,200 descriptors

generated from 1D, 2D and 3D parameters were combined with electronic descriptors from quantum chemical calculations. These descriptors were pre-treated for carefully selected of relevant parameters to avoid multicollinearity using Data Pre-Treatment GUI 1.2" tool, which utilizes the V-WSP algorithm to eliminate these descriptors and ensure the reliability and generalization of the subsequent QSAR modelling. These data were split into training set (70%) for the QSAR model development and test set (30%) for validation of the model using Dataset Division GUI tool version 1.2 in a random manner as implemented in Drug Theoretical and Cheminformatics Laboratory (DTC Lab) software . The QSAR model was constructed using the compounds from the training set. The independent variables (descriptors) were correlated to the dependent variable (pIC50 of **A549** through multivariate analysis using the Genetic Algorithms Function Approximation (GAFA) technique in the DTC Lab software (Mahmud et al., 2020). The fitness of the model was assessed during the evolution process using the Friedman lack-of-fit (LOF) measure. In Material Studio, the LOF value is calculated using equation 2. The developed QSAR models were validated to test the internal stability and predictive ability of the models. The procedure employed in model validation is internal and external validation (Islam et al., 2014; Oyebamiji et al., 2016; Abdullah et al., 2020).

(i) Friedman

$$LOF = SSE \left( 1 - \frac{c+dp}{M} \right)^2 \quad (2)$$

where SSE is the sum of squares of errors, c is the number of terms in the model, other than the constant term, d is a user-defined smoothing parameter, p is the total number of descriptors contained in all model terms (again ignoring the constant term) and M is the number of samples in the training set (Isyaku et al., 2020).

(ii)

$$SSE \left( \sqrt{\frac{(Y_{obs} - Y_{pred})^2}{N - P - 1}} \right) \quad (3)$$

(ii) R-squared ( $R^2$ ) is determined by equation 4

$$R^2 = \frac{\left( \sum \{ [Y_{obs} - \bar{Y}_{tr}] / [Y_{pred} - \bar{Y}_{pred}] \} \right)^2}{\sum (Y_{obs} - \bar{Y}_{tr})^2 \sum (Y_{pred} - \bar{Y}_{pred})^2} \quad (4)$$

(iii) Cross validated R squared ( $Q^2_{cv}$ ) is estimated using equation 5

$$Q^2_{cv} = 1 - \frac{\sum (Y_{pred} - Y_{Obs})^2}{\sum (Y_{obs} - \bar{Y}_{tr})^2} \quad (5)$$

$Y_{pred}$  and  $Y_{obs}$  are predicted and observed training set concentration (experimental), respectively.  $\bar{Y}_{tr}$  and  $\bar{Y}_{pred}$  are the average observed (experimental) and predicted training set response, respectively.

(iii) Coefficient of determination adjusted ( $R^2$  adjusted) is determined using equation 6

$$R^2_{adj} = \frac{R^2 - p(n-1)}{n-1-p} \quad (6)$$

where  $p$  = number of the descriptor in the model,  $n$  = number of compounds in the training set,  $R^2$  is the correlation coefficient, and  $n-1-p$  is the degree of freedom.

### Docking of the Protein-Ligand

The X-ray structure of the A549 protein target (PDB ID: 7MLR) was retrieved from protein data bank (www.rcsb.org). It was purified and repaired using discovery Studio Visualizer version 16.1.0.15350 and Avogadro. The protein and optimized structures of the ligands were saved in PDB format and molecular docking was performed using PyRx software; the docking results were analysed with discovery Studio Visualizer version [47, 39].

*In-silico ADMET/Pharmacokinetic Predictions*

The pKCSM online tool software was utilized to predict the pharmacokinetic properties (<http://bi-osisg.unimelb.edu.au/pkCSM/prediction>), specifically the ADMET (Absorption, Distribution, Metabolism, Excretion, and Toxicity), of the compounds [48].

**Results and discussion***Molecular descriptors and Docking analysis.*

The quantum chemical descriptors of triazole-trimethoxyphenyl hybrids obtained from B3LYP/6-31G(d,p) method are provided in Table 2. The HOMO energies for the triazole-trimethoxyphenyl hybrids ranged from -5.40 eV (TPD 25) to -8.69 eV (TPD 13), suggesting that TPD 11 and TPD 25 have higher propensity to donate electrons to the protein receptor, particularly to the electron acceptor hydrogen and carbon atoms within the receptor [49]. The LUMO and chemical potential energies ( $\mu$ ) of TPD 11 (-1.98 and -3.75 eV) and TPD 25 (-1.98 and -3.69 eV), respectively, are lower than that of Etoposide (-0.10 and -2.72 eV), indicating that TPD 11 and TPD 25 can readily receive electrons from the surrounding (protein) than Etoposide [50, 51]. Also, dipole moment (7.44 and 4.96 Debye), HOMO-LUMO energy gap ( $\Delta E_g$ , 3.53 and 3.42 eV), chemical hardness (1.77 and 1.71 eV) and softness (0.565 and 0.585 eV<sup>-1</sup>) favour interactions of TPD 11 and TPD 25, respectively, with protein than Etoposide [52 - 55]. This was in agreement with IC<sub>50</sub> of 0.69 and 0.60 of TPD 11 and TPD 25, respectively compared to 2.99  $\mu$ M for Etoposide, as observed against adenocarcinomic human alveolar basal epithelial cells, A549 (Ansari et al., 2019) as presented in Table 1. Thus, TPD 11 and TPD 25 are expected to engage in hydrogen bonding and other hydrophobic interactions with a receptor more than Etoposide which may lead to enhance binding properties with the receptor [56].

Table 2: Molecular parameters calculated from DFT-B3LYP/6-31G(d,p) for the compounds

CPD	<i>H</i> (eV)	<i>L</i> (eV)	$\Delta E_g$	Dipole moment (Debye)	$\mu$ (eV)	$\eta$ (eV)	$S = 1/\eta$	$\omega$ (eV)
TPD-1	-5.93	-2.02	3.91	6.61	-3.98	1.96	0.510	4.04
TPD-2	-5.65	-2.11	3.54	6.17	-3.88	1.77	0.565	4.25
TPD-3	-5.54	-1.99	3.55	5.79	-3.77	1.78	0.562	3.99
TPD-4	-5.46	-1.98	3.48	5.88	-3.72	1.74	0.575	3.98
TPD-5	-6.26	1.90	8.16	6.38	-2.18	4.08	0.245	0.58
TPD-6	-6.16	-2.08	4.08	7.02	-4.12	2.04	0.490	4.16
TPD-7	-6.46	-1.98	4.48	6.17	-4.22	2.24	0.446	3.98
TPD-8	-5.89	-2.07	3.82	8.43	-3.98	1.91	0.524	4.15
TPD-9	-5.76	-2.04	3.72	8.49	-3.90	1.86	0.538	4.09
TPD-10	-5.55	-2.02	3.53	6.93	-3.79	1.77	0.565	4.06
TPD-11	-5.51	-1.98	3.53	7.44	-3.75	1.77	0.565	3.97
TPD-12	-5.47	-1.86	3.61	7.21	-3.67	1.81	0.553	3.72
TPD-13	-8.69	1.56	10.25	10.65	-3.57	5.13	0.195	1.24
TPD-14	-5.66	-2.23	3.43	4.35	-3.95	1.72	0.581	4.54
TPD-15	-8.18	1.72	9.90	5.39	-3.23	4.95	0.202	1.05
TPD-16	-5.54	-1.91	3.63	6.29	-3.73	1.82	0.550	3.82
TPD-17	-5.64	-1.97	3.67	4.93	-3.81	1.84	0.544	3.94
TPD-18	-5.65	-2.01	3.64	5.15	-3.83	1.82	0.550	4.03
TPD-19	-5.67	-2.14	3.53	3.85	-3.91	1.77	0.565	4.32
TPD-20	-5.67	-2.17	3.50	4.13	-3.92	1.75	0.571	4.39
TPD-21	-5.70	-2.99	2.71	3.31	-4.35	1.36	0.735	6.97
TPD-22	-5.72	-2.30	3.42	3.28	-4.01	1.71	0.585	4.70

TPD-23	-5.63	-1.93	3.70	5.68	-3.78	1.85	0.540	3.86
TPD-24	-5.56	-1.92	3.64	6.92	-3.74	1.82	0.550	3.84
TPD-25	-5.40	-1.98	3.42	4.96	-3.69	1.71	0.585	3.98
TPD-26	-5.61	-2.16	3.45	5.76	-3.89	1.73	0.578	4.37
Etoposide	-5.34	-0.10	5.24	3.53	-2.72	2.62	0.382	1.41

The analysis of docking results showed that the binding affinities ranged from -6.8 kcal/mol (TPD-7) to -8.6 kcal/mol (TPD-25). The triazole-trimethoxyphenyl hybrids with higher binding affinities against adenocarcinomic human alveolar basal epithelial cells, A549 (ID: 7MLR) are TPD-10 and TPD-14 (-8.0 kcal/mol), TPD-19 (-8.4 kcal/mol), TPD-20, TPD-21 and TPD-26 (-8.5 kcal/mol) and TPD-25 (-8.6 kcal/mol). TPD-10 and TPD-14 are hydrogen bonded with ILE 146; TPD-19 is hydrogen bonded with GLN 85 and PRO 86; TPP 20 is hydrogen bonded with GLN 85, TYR 97, ASN 140 and ILE 146; TPD-21 is hydrogen bonded with GLN 85; TPD-26 is hydrogen bonded with ASP 144 and ASN 140; while TPD-25 is hydrogen bonded with ASN 140, ILE 146 and CYS 137. The binding affinity of Etoposide is -8.8 kcal/mol having hydrogen binding with ASN 140 and PRO 86 (Table 3). The TPD-25 with highest inhibitory activity against adenocarcinomic human alveolar basal epithelial cells, A549 (Table 1), also presented highest binding affinity among the triazole-trimethoxyphenyl hybrids, thus it is used as QSAR reference compound for modelling and prediction of IC<sub>50</sub> for new triazole-trimethoxyphenyl hybrids in this work.

Table 3: Binding affinities (kcal/mol) of the 26 triazole-trimethoxyphenyl hybrids with **A549 (ID: 7MLR)**

CPD	RECEPTOR A549			
	Binding affinity $\Delta G$ (Kcalmol <sup>-1</sup> )	Inhibition constant $K_i$ ( $\mu$ M)	H-BOND with ligands	H bond distance(Å)
TPD-1	-7.7	2.25	GLN 85	2.41
			PRO 86	3.77
TPD-2	-7.4	3.74	PRO 86, GLN 85	3.37, 2.08
			ASP 88	1.79
			PRO 82	2.15
			GLN 85	3.54
TPD-3	-7.6	2.67	GLN 85	2.35
			ASN 140	2.23
			MET 105	2.39
TPD-4	-7.7	2.25	GLN5 8	2.35
TPD-5	-7.3	4.43	ASN 140	2.32
			GLN 85	2.82
			MET 105	3.70
			PRO 86	3.36
TPD-6	-7.0	7.35	ASN140	2.65
TPD-7	-6.8	10.30	PRO 82	3.73
TPD-8	-7.9	1.61	ILE 146	2.67
TPD-9	-7.9	1.61	ILE 146	2.62
TPD-10	-8.0	1.36	ILE 146	2.60

TPD-11	-7.5	3.16	Nil	Nil
TPD-12	-7.8	1.90	ILE 146	2.78
TPD-13	-7.8	1.90	ILE 146	2.84
TPD-14	-8.0	1.36	ILE 146	2.60
TPD-15	-7.9	1.61	GLN 85, PRO 86	2.08, 3.37
TPD-16	-7.6	2.67	ILE 146, MET 105, MET 132	2.51, 3.19, 3.54
TPD-17	-7.8	1.90	GLN 85, TYR 97, MET 105, PRO 86, ASN 135	2.23, 2.42, 3.57, 3.23, 3.79
TPD-18	-6.8	10.30	GLN 85, ASN 140, PRO 86	2.36, 2.56, 3.35
TPD-19	-8.4	0.69	GLN 85, PRO 86	2.10, 3.52
TPD-20	-8.5	0.58	GLN 85, TYR 97, ASN 140, ILE 146	2.78, 2.15, 2.48, 3.71
TPD-21	-8.5	0.58	GLN 85	2.14
TPD-22	-7.5	3.16	GLN 85	2.45
TPD-23	-7.5	3.16	MET 132	2.50
			ILE 146	2.96
TPD-24	-7.5	3.16	ASN 140	2.45
			ILE 146	2.17
			CYS 136	2.72
TPD-25	-8.6	0.49	ASN 140	2.45
			ILE 146	2.72
			CYS 137	3.36
TPD-26	-8.5	0.58	ASP 144	3.51
			ASN 140	3.64
Etoposide	-8.8	0.35	ASN 140	2.99
			PRO 86	3.77

#### QSAR model using Multilinear Regression Genetic Algorithm (MLR-GFA)

The QSAR model developed via MLR-GFA, as shown in equation 7, of inhibitory activity ( $pIC_{50} = -\log (IC_{50})$ ) of triazole-trimethoxyphenyl hybrids against adenocarcinomic human alveolar basal epithelial cells (A549) contains four independent 2D-molecular descriptors. These descriptors symbols and definitions are displayed in Table 4.

$$pIC_{50} = 0.3773 - 6.4175 * MATS4p + 0.3043 * minHBint3 + 0.5099 * ATSC7c - 0.1974 * naasC \quad (7)$$

QSAR model displayed a negative contribution from MATS4p and naasC descriptors, while minHBint3 and ATSC7c descriptors contributed positively. Thus, increase in MATS4p and naasC values will negatively influence the predicted value of  $pIC_{50}$ , meanwhile, minHBint3 and ATSC7c descriptors will have positive impact on the model. Figure 2 shows the percentage contributions of each descriptor to the predicted  $pIC_{50}$ . The Pearson correlation analysis of the descriptor and  $pIC_{50}$



values of the model shows nonexistence of inter-correlation among the descriptors as displayed in Table 5.

Table 4: Symbols definitions and descriptors used in the MLR-GFA equation.

S/N	Descriptor	Definition	Class	Contribution
1	MATS4p	Moran autocorrelation - lag 4 / weighted by polarizabilities.	2D	Negative
2	ATSC7c	Centered Broto-Moreau autocorrelation - lag 7 / weighted by charges.	2D	Positive
3	minHBint3	Minimum E-State descriptors of strength for potential Hydrogen Bonds of path length 3	2D	Positive
4	naasC	Count of atom-type E-State: C:	2D	Negative

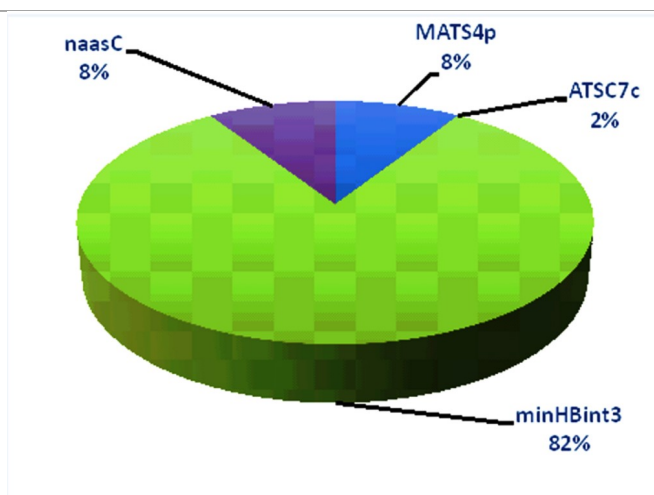


Figure 2: Pie chart showing the Influence of each descriptor in the Model.

Table 5: Table of correlation matrix for the descriptors.

	pIC <sub>50</sub>	MATS4p	ATSC7c	minHBint3	naasC
pIC <sub>50</sub>	1				
MATS4p	0.074446	1			
ATSC7c	-0.00223	0.414277	1		
minHBint3	0.663251	0.595809	0.184444	1	
naasC	0.075153	-0.29125	0.07373	0.282719	1

The model is statistically validated with  $R$ -squared ( $R^2$ ), adjusted  $R^2$ , Cross validated  $R$  squared ( $Q^2$ ) are 0.8632, 0.7951 and 0.6023, respectively. The model general robustness is also examined using the differences in  $R^2$  and  $Q^2_{cv}$  which is  $< 0.3$  and Friedman  $LOF$  is 0.001 (Table 6). The inter-correlated descriptor characteristics of model are evaluated based on their multicollinearity estimated using the variation inflation factor ( $VIF$ ) as shown in equation 8.

$$VIF = (1 - R^2)^{-1} \quad (8)$$

In this case,  $R^2$  is the correlation coefficient, and  $VIF$  value approaching a unity, is an indication of no inter-correlation among each descriptor in the model. The  $VIF$  scores between 1 and 5 means the model is within acceptability and stability arena; nevertheless, if the  $VIF$  score  $> 10$ , then the model is unstable and unacceptable [57]. The  $VIF$  scores in Figure 3 shows that the model is stable and acceptable, thus the model can be used to predict bioactivity ( $pIC_{50}$ ) of similar triazole-trimethoxyphenyl hybrids against adenocarcinomic human alveolar basal epithelial cells (A549).

Table 6: QSAR validation parameters

S/N	Parameter	Threshold value	Computed value	Statement
1	R-squared ( $R^2$ )	> 0.6	0.8146	Good
2	Adjusted $R^2$ ( $R^2_{adj}$ )	> 0.6	0.7874	Good
4	Cross validated R squared ( $Q^2$ )	> 0.5	0.6015	Good
5	Friedman LOF	< 0.1	0.0246	Good
6	$R^2 - Q^2_{LOO}$	< 0.3	0.2582	Good

The experimental  $IC_{50}$  ( $pIC_{50}$ ) of TPDs against A549 reported by Ansari et al., [35] and the predicted  $pIC_{50}$  and the residual values (difference between the experimental  $pIC_{50}$  and predicted  $pIC_{50}$ ) are displayed in Table 7. The lower residual score implies that the model has good predictive potential. Figures 3 and 4 display the observed versus predicted activity and residual plots, demonstrating the accuracy of the model with  $R_{pred}^2$  of 0.8632, which is greater than 0.6 threshold value.

Table 7: The experimental and predicted  $pIC_{50}$  of the ligands.

Ligand	Experimental	Predicted	
	$pIC_{50}$ ( $\mu M$ )	$pIC_{50}$ ( $\mu M$ )	Residual
<b>TPD 1*</b>	<b>-0.60</b>	<b>-0.45</b>	<b>-0.15</b>
TPD 2	-0.64	-0.59	-0.05
TPD 3	-0.62	-0.57	-0.05
TPD 4	-0.57	-0.52	-0.05
<b>TPD 5*</b>	<b>-0.41</b>	<b>-0.37</b>	<b>-0.04</b>
TPD 6	-0.45	-0.44	-0.01
<b>TPD 7*</b>	<b>-0.58</b>	<b>-0.47</b>	<b>-0.11</b>
TPD 8	-0.57	-0.52	-0.05
<b>TPD 9*</b>	<b>-0.66</b>	<b>-0.72</b>	<b>0.06</b>
TPD 10	-0.62	-0.55	-0.07
<b>TPD 11*</b>	<b>0.17</b>	<b>0.23</b>	<b>-0.06</b>
TPD 12	-0.51	-0.43	-0.08
<b>TPD 13*</b>	<b>-0.60</b>	<b>-0.75</b>	<b>0.15</b>
TPD 14	-0.44	-0.53	0.09
<b>TPD 15*</b>	<b>-0.02</b>	<b>-0.09</b>	<b>0.07</b>
TPD 16	-0.56	-0.44	-0.12
TPD 17	-0.40	-0.62	0.22
TPD 18	-0.60	-0.54	-0.06
<b>TPD 19*</b>	<b>-0.45</b>	<b>-0.27</b>	<b>-0.18</b>
<b>TPD 20*</b>	<b>-0.33</b>	<b>-0.22</b>	<b>-0.11</b>
TPD 21	-0.70	-0.43	-0.27
TPD 22	-0.50	-0.57	0.07
TPD 23	-0.70	-0.67	-0.03

TPD 24	-0.51	-0.46	-0.05
TPD 25	0.22	0.28	-0.06

Note \* test set for the cancer cell line.

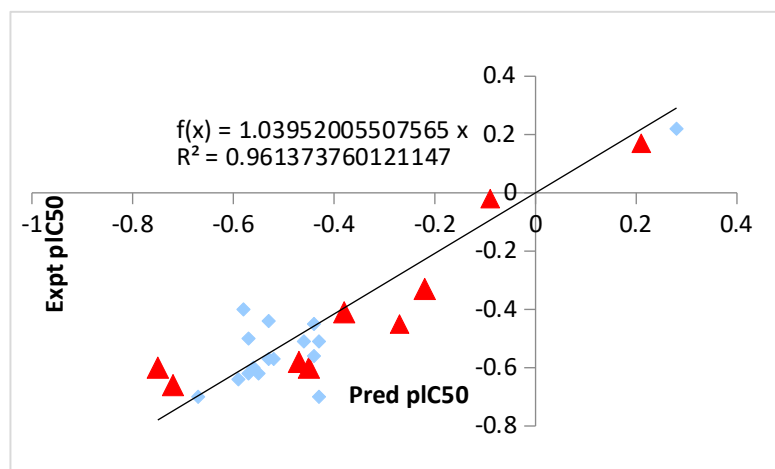


Figure 3: Graph of internal validation for MLR-GFA (Test in red)

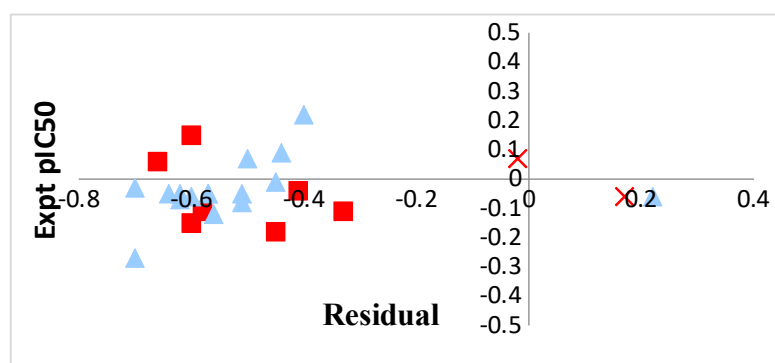
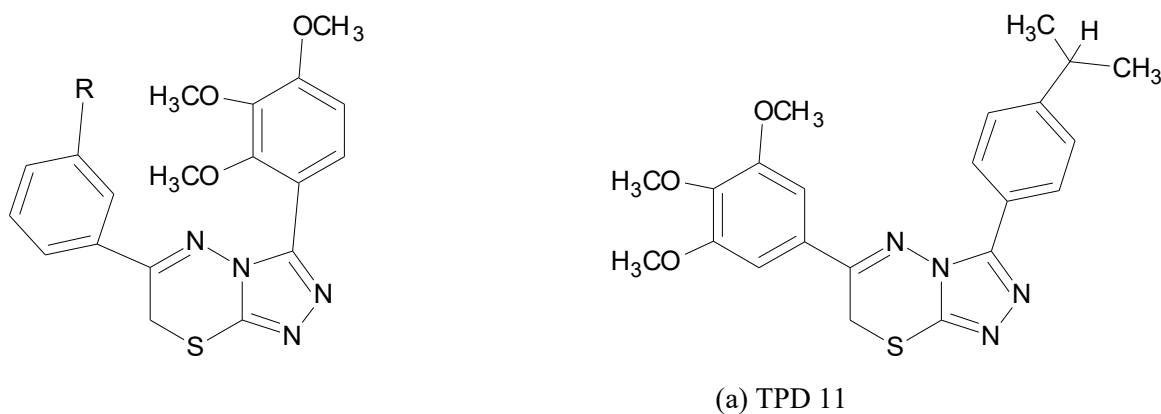


Figure 4: Graph of Residual plot for A549- MLR-GFA model, Test in red

#### Design of new triazole-trimethoxyphenyl hybrids and their computed $pIC_{50}$ values

New twenty-eight molecules with their computed  $pIC_{50}/IC_{50}$  values were predicted, from which the best ten were selected in all out of which eight were from TPD-25 (NTPD-1 to NTPD-8) and other two from TPD-11 (NTPD-9 and NTPD-10) as shown in Figure 5. The compounds TPD-11 and TPD-25 were selected as lead molecules based on experimental bioactivity against adenocarcinomic human alveolar basal epithelial cells (Table 1). The new molecules with outstanding  $IC_{50}$  than Etoposide ( $2.99 \mu M$ ) are NTPD-3 ( $0.594 \mu M$ ), NTPD-4 ( $0.813 \mu M$ ), NTPD-6 ( $1,514 \mu M$ ), NTPD-8 ( $2,743 \mu M$ ) and NTPD-9 ( $1.090 \mu M$ ).



S/N	R	Name	pIC <sub>50</sub>	IC <sub>50</sub>
NTPD-1	CH <sub>2</sub> CH <sub>3</sub>	3-(4-ethylphenyl)-6-(3,4,5-trimethoxyphenyl)-7H-[1,2,4]triazolo[3,4-b][1,3,4]thiadiazine, 0.997	-0.878	7.56
NTPD-2	CH(CH <sub>3</sub> ) <sub>2</sub>	3-(3-(propan-2-yl)phenyl)-6-(3,4,5-trimethoxyphenyl)-7H-[1,2,4]triazolo[3,4-b][1,3,4]thiadiazine	-0.467	2.93
NTPD-3	C(CH <sub>3</sub> ) <sub>3</sub>	3-(3-tert-butylphenyl)-6-(3,4,5-trimethoxyphenyl)-7H-[1,2,4]triazolo[3,4-b][1,3,4]thiadiazine	0.226	0.59
NTPD-4	OCH <sub>2</sub> CH <sub>3</sub>	3-(3-ethoxyphenyl)-6-(3,4,5-trimethoxyphenyl)-7H-[1,2,4]triazolo[3,4-b][1,3,4]thiadiazine	0.090	0.81
NTPD-5	S-CH <sub>3</sub>	3-(3-methylsulfanylphenyl)-6-(3,4,5-trimethoxyphenyl)-7H-[1,2,4]triazolo[3,4-b][1,3,4]thiadiazine	-0.719	5.24
NTPD-6	NO <sub>2</sub>	3-(3-nitrophenyl)-6-(3,4,5-trimethoxyphenyl)-7H-[1,2,4]triazolo[3,4-b][1,3,4]thiadiazine	0.180	1.51
NTPD-7	CN	3-(3-cyanophenyl)-6-(3,4,5-trimethoxyphenyl)-7H-[1,2,4]triazolo[3,4-b][1,3,4]thiadiazine	-0.346	2.22
NTPD-8	NH <sub>2</sub>	3-(3-aminophenyl)-6-(3,4,5-trimethoxyphenyl)-7H-[1,2,4]triazolo[3,4-b][1,3,4]thiadiazine	-0.438	2.74
NTPD-9	O-CH <sub>3</sub>	6-(3-methoxyphenyl)-3-(2,3,4-trimethoxyphenyl)-7H-[1,2,4]triazolo[3,4-b][1,3,4]thiadiazine	-0.037	1.09
NTPD-10	S-CH <sub>3</sub>	6-(3-methylsulfanylphenyl)-3-(2,3,4-trimethoxyphenyl)-7H-[1,2,4]triazolo[3,4-b][1,3,4]thiadiazine	-0.624	4.21

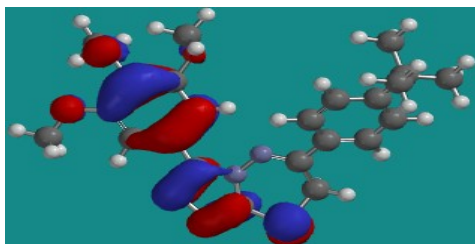
Figure 5: 2-D structures, IUPAC names bioactivity of new triazole-trimethoxyphenyl hybrids against adenocarcinomic human alveolar basal epithelial cells (A549)

The frontier energies and reactivity descriptors of the four compounds, NTPD-3, NTPD-4, NTPD-6 and NTPD-9 (out of ten new compounds) with outstanding predicted bioactivity against adenocarcinomic human alveolar basal epithelial cells (A549) are listed in Table 8 with orbital overlay in Figure 6. The LUMO and chemical potential ( $\mu$ ) energies of these compounds showed that they can readily receive electrons from the surrounding (protein) than Etoposide [51]. Also,  $\Delta E_g$ , chemical hardness ( $\eta$ ), and softness favour interactions of valence electrons of these compounds with adenocarcinomic human alveolar basal epithelial cells (A549). However, the HOMO supports the ease of electron donating ability of Etoposide with the protein than these new compounds [53]; thus, Etoposide is expected to donate electrons to the protein readily than these NTPD compounds. The molecular docking analysis of predicted NTPD compounds showed that binding affinity for NTPD-3, NTPD-4, NTPD-6 and NTPD-9 are -7.9, -7.5, -8.0 and -7.8 kcalmol<sup>-1</sup>, respectively, as compared to -8.8 kcalmol<sup>-1</sup> for Etoposide (Figure 7).

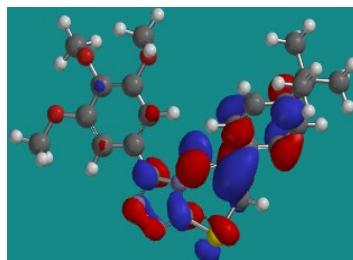
Table 8: Chemical descriptors calculated for new predicted triazole -trimethoxyphenyl hybrids

CPD	H (eV)	L (eV)	$\Delta E_g$	Dipole Moment (Debye)	CPD	H (eV)	L (eV)	$\Delta E_g$
NTPD-3	-5.59	-2.00	3.59	5.95	-3.795	1.795	0.557	4.012
NTPD-4	-5.56	-1.89	3.67	6.22	-3.725	1.835	0.545	3.781
NTPD-6	-5.86	-3.11	2.75	1.50	-4.485	1.375	0.727	7.315

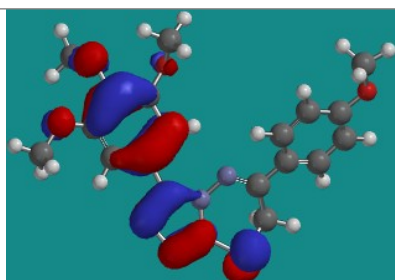
NTPD-9	-5.81	-2.02	3.79	6.41	-3.915	1.895	0.528	4.044
<b>Etoposide</b>	-5.34	-0.10	5.24	3.53	-2.720	2.620	0.382	1.412



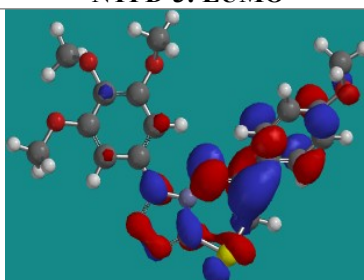
**NTPD-3: HOMO**



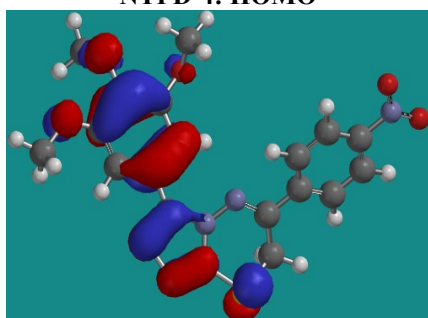
**NTPD-3: LUMO**



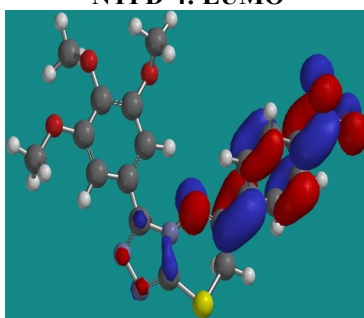
**NTPD-4: HOMO**



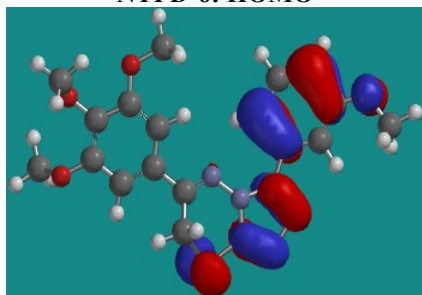
**NTPD-4: LUMO**



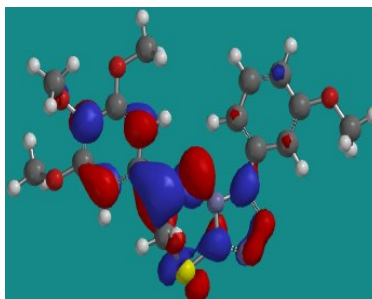
**NTPD-6: HOMO**



**NTPD-6: LUMO**



**NTPD-9: HOMO**



**NTPD-9: LUMO**

Figure 6: The frontier orbitals overlaid diagram of new triazole -trimethoxyphenyl hybrids

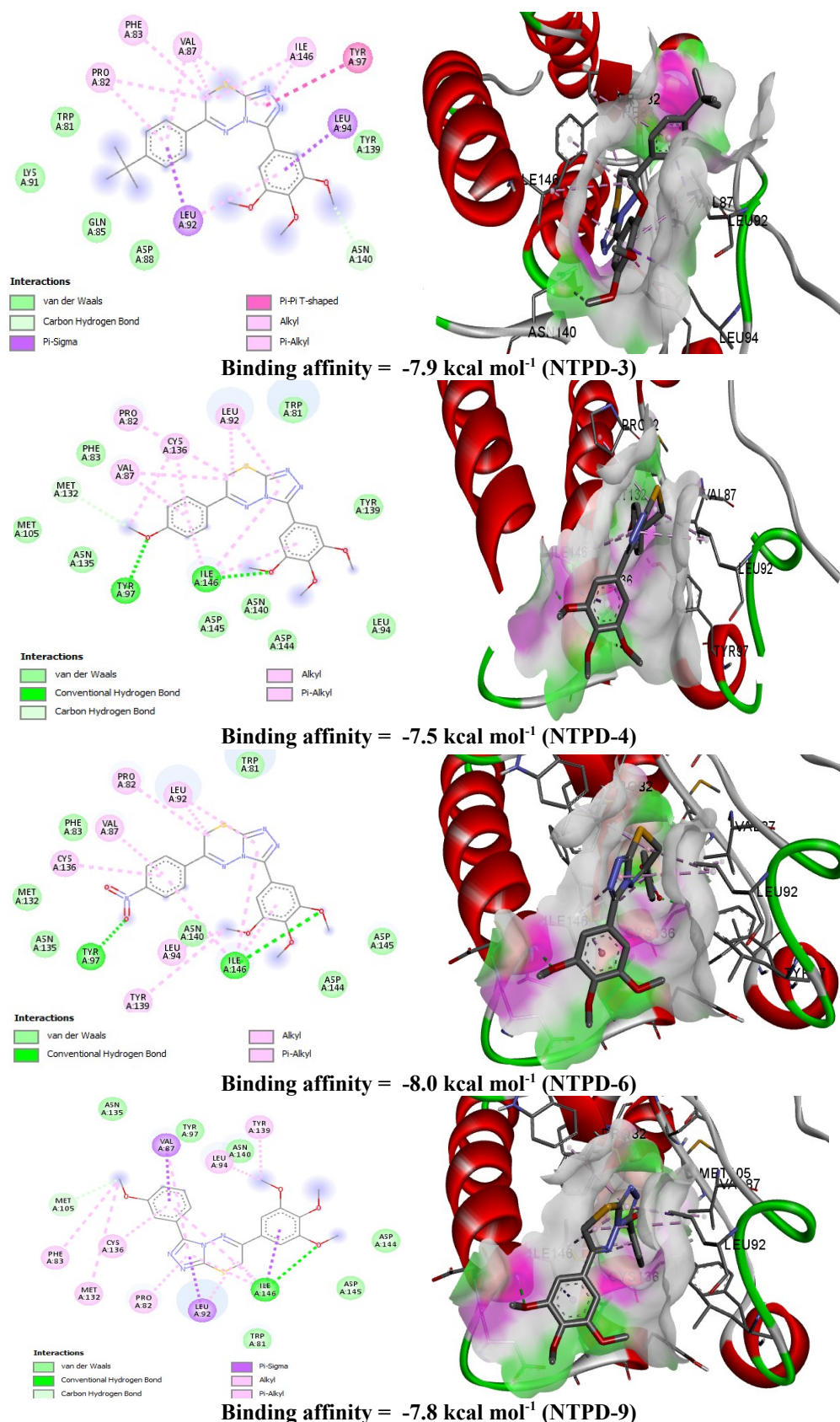


Figure 7: binding affinity and 2-D diagram of the newly designed ligands with A549 (ID: 7MLR).

The assessment of drug likeness and oral bioavailability is crucial, especially for orally administered drugs. Lipinski's Rule of Five is a widely accepted guideline in this context. The rule states that a molecule should not violate more than one of the following parameters: molecular weight



(Mw) < 500, number of hydrogen bond donors (HBD) < 5, octanol/water partition coefficient (log P) < 5, and number of hydrogen bond acceptors (HBA) < 10. The physicochemical properties of the new designed triazole-trimethoxyphenyl hybrids against adenocarcinomic human alveolar basal epithelial cells indicated that these compounds adhere to Lipinski's rule except NTPD-6 with one violation. The ADMET properties predicted for these new compounds showed that NTPD-6 displayed good oral absorption, water solubility, skin permeability, non P-glycoprotein substrate which may enhance bioavailability. Blood-brain barrier (BBB) permeability predictions indicated that the ligands could cross the BBB, but they showed low permeability, indicating moderate distribution to the central nervous system (CNS). The ligand acted as non-inhibitor of human cytochrome P450 enzymes, especially CYP1A2, CYP2C19, CYP2C9 and CYP2D6 (Table 10). This suggests that it may undergo metabolic transformations. The ligands exhibit low Oral- Rat Chronic toxicity (LOAEL), Hepatotoxicity and Skin sensitization total clearance values, suggesting prolonged stability in the body and enhanced drug efficacy.

Table 10: ADMET properties of the predicted ligands.

Property	Model Name	NTPD-3	NTPD-4	NTPD-6	NTPD-9	Etoposide
ABSORPTION	H <sub>2</sub> O solubility	-5.648	-4.195	-4.399	-4.288	-3.69
	Caco-2 Permeability	1.458	1.215	0.732	1.361	0.56
	Intestinal absorption (human)	97.24	99.147	93.742	99.836	91.44
	Skin permeability	-2.741	-2.739	-2.746	-2.744	-2.74
	P- glycoprotein substrate	No	No	No	No	Yes
	P-glycoprotein I inhibitor	Yes	Yes	Yes	Yes	No
	P-glycoprotein II inhibitor	Yes	Yes	No	Yes	No
DISTRIBUTION	VDSS (human)	0.015	-0.126	-0.193	-0.152	0.42
	Fraction on bound (human)	0.009	0.072	0.098	0.064	0.11
	BBB permeability	-1.009	-1.263	-1.393	-1.281	-1.61
	CNS permeability	-1.962	-3.489	-3.402	-3.254	-3.71
METABOLISM	CYP2D6 Substrate	No	No	No	No	NO
	CYP3A4 Substrate	Yes	Yes	Yes	Yes	NO
	CYP1A2 inhibitor	Yes	Yes	No	Yes	NO
	CYP2C19 inhibitor	Yes	Yes	No	Yes	NO
	CYP2C9 inhibitor	Yes	Yes	No	Yes	NO
	CYP2D6 inhibitor	No	No	No	No	NO
	CYP3A4 inhibitor	Yes	Yes	Yes	Yes	NO
EX-CREATION	Total clearance	0.585	0.596	0.61	0.783	0.00
	Renal OCT2 substrate	No	No	No	No	NO
TOXICITY	AMES toxicity	No	No	No	No	NO
	Max. tolerated dose (human)	0.541	0.627	0.668	0.532	0.10
	hERG I inhibitor	No	No	No	No	NO
	hERG II inhibitor	Yes	Yes	No	Yes	NO
	Oral- Rat Acute toxicity (LD <sub>50</sub> )	2.752	2.845	2.427	2.648	3.00
	Oral- Rat Chronic toxicity (LOAEL)	1.266	1.365	0.97	1.34	2.94
	Hepatotoxicity	Yes	Yes	No	Yes	NO
	Skin sensitization	No	No	No	No	NO
	T. Pyriformis toxicity	0.31	0.294	0.287	0.3	0.29
	Minnow toxicity	-0.215	-1.432	-1.443	-0.715	5.08

## Conclusion

*In silico* methods were used to evaluate twenty-six triazole-trimethoxyphenyl hybrids anticancer activity against adenocarcinomic human alveolar basal epithelial cells (A549) through DFT, QSAR and ADMET profile. The DFT results showed that TPD 11 and TPD 25 have better molecular properties to receive electrons from and donate electrons to adenocarcinomic human alveolar basal epithelial cells readily than Etoposide. Thus, they are expected to engage in hydrogen bonding and other hydrophobic interactions with a receptor more than Etoposide which led to enhance binding properties. The QSAR developed using multiple linear regression-Genetic Approximation (MLR-GA) statistically has very good predictive ability, which was used to predict twenty-eight molecules of which NTPD-3, NTPD-4 NTPD-6 and NTPD-9 have computed pIC<sub>50</sub>/IC<sub>50</sub> values better than etoposide. The physicochemical and ADMET properties showed that NTPD-6 displayed good oral absorption, water solubility, skin permeability, non-P-glycoprotein substrate, exhibited low Oral- Rat Chronic toxicity (LOAEL), Hepatotoxicity and Skin sensitization total clearance values, suggesting it could be a good candidate inhibitor against adenocarcinomic human alveolar basal epithelial cells.

## Acknowledgements

Authors acknowledged the staff of Computational Chemistry Laboratory, Department of Pure and Applied Chemistry of Ladoke Akintola University of Technology, Ogbomosho, Nigeria for granting us access to their computational resources.

## References

1. Budrevičiūtė, A.; Damiani, S.; Sabir, D.K.; Önder, K.; Schuller-Goetzburg, P.; Plakys, G.; Katileviciute, A.; Khoja, S.M.; Kodzius, R.; Management and Prevention Strategies for Non-communicable Diseases (NCDs) and their risk factors, *Frontiers in Public Health*. **2020**, *8*, <https://doi.org/10.3389/fpubh.2020.574111>.
2. World Health Organization: WHO, Noncommunicable diseases, **2023**. <https://www.who.int/news-room/fact-sheets/detail/noncommunicable-diseases>.
3. Ferlay, J.; Colombet, M.; Soerjomataram, I.; Parkin, D.M.; Piñeros, M.; Znaor, A.; Bray, F.; Cancer statistics for the year 2020: An overview, *International Journal of Cancer*. **2021**, *149*, 778–789. <https://doi.org/10.1002/ijc.33588>.
4. Muka, T.; Imo, D.; Jaspers, L.; Colpani, V.; Chaker, L.; Van Der Lee, S.J.; Mendis, S.; Chowdhury, R.; Bramer, W.M.; Falla, A.; Pazoki, R.; Franco, O.H.; The global impact of non-communicable diseases on healthcare spending and national income: a systematic review, *European Journal of Epidemiology*. **2015**, *30*, 251–277. <https://doi.org/10.1007/s10654-014-9984-2>.
5. Ullrich, A.; Miller, A.B.; Global Response to the Burden of Cancer: The WHO approach, *American Society of Clinical Oncology Educational Book*. **2014**, e311–e315. [https://doi.org/10.14694/edbook\\_am.2014.34.e311](https://doi.org/10.14694/edbook_am.2014.34.e311).
6. Nikolaou, M.; Pavlopoulou, A.; Georgakilas, A.G.; Kyrodimos, E.; The challenge of drug resistance in cancer treatment: a current overview, *Clinical & Experimental Metastasis*. **2018**, *35*, 309–318. <https://doi.org/10.1007/s10585-018-9903-0>.
7. Özkan, S.A.; Advances in Medicinal Chemistry from Analytical Perspectives, *Current Medicinal Chemistry*. **2018**, *25* 3954–3955.
8. Palve, V.; Liao, Y.W.; Rix, L.; Rix, U.; Turning liabilities into opportunities: Off-target based drug repurposing in cancer, *Seminars in Cancer Biology*. **2021**, *68*, 209–229. <https://doi.org/10.1016/j.semcancer.2020.02.003>.
9. Fu, D.-J.; Yang, J.; Li, P.; Hou, Y.; Huang, S.; Tippin, M.; Pham, V.; Song, L.; Zi, X.; Xue, W.; Zhang, L.; Zhang, S.; Bioactive heterocycles containing a 3,4,5-trimethoxyphenyl fragment exerting potent antiproliferative activity through microtubule destabilization, *European Journal of Medicinal Chemistry*. **2018**, *157*, 50–61. <https://doi.org/10.1016/j.ejmech.2018.07.060>.
10. Lang, D.K.; Kaur, R.; Arora, R.; Saini, B.; Arora, S.; Nitrogen-Containing heterocycles as Anticancer agents: An Overview, *Anti-Cancer Agents in Medicinal Chemistry*. **2020**, *20*, 2150–2168.



11. Kerru, N.; Gummidi, L.; Maddila, S.; Gangu, K.K.; Jonnalagadda, S.B.; A review on recent advances in Nitrogen-Containing molecules and their biological applications, *Molecules*. **2020**, *25*, 1909. <https://doi.org/10.3390/molecules25081909>.
12. Al-Bayati, A.I.; Mahmood, A. A. R.; Tahtamouni, L.H.; Al-Mazaydeh, Z.A.; Rammaha, M.S.; Al-Bayati, R.I.; Alsoubani, F.; WITHDRAWN: Synthesis, docking study, and in-vitro anti-cancer evaluation of new triazole derivatives of flufenamic. <https://doi.org/10.1016/j.matpr.2021.05.317>. acid, *Materials Today: Proceedings*. **2021**
13. Zhao, S.; Liu, J.; Lv, Z.; Zhang, G.; Xu, Z.; Recent updates on 1,2,3-triazole-containing hybrids with in vivo therapeutic potential against cancers: A mini-review, *European Journal of Medicinal Chemistry*. **2023**, *251*, 115254. <https://doi.org/10.1016/j.ejmech.2023.115254>.
14. Grytsai, O.; Valiashko, O.; Penco-Campillo, M.; Dufies, M.; Hagege, A.; Demange, L.; Martial, S.; Pagès, G.; Ronco, C.; Benhida, R.; Synthesis and biological evaluation of 3-amino-1,2,4-triazole derivatives as potential anticancer compounds, *Bioorganic Chemistry*. **2020**, *104*, 104271. <https://doi.org/10.1016/j.bioorg.2020.104271>.
15. Chu, X.; Wang, C.; Wang, W.; Liang, L.; Liu, W.; Gong, K.; Sun, K.; Triazole derivatives and their antiplasmodial and antimalarial activities, *European Journal of Medicinal Chemistry*. **2019**, *166*, 206–223. <https://doi.org/10.1016/j.ejmech.2019.01.047>.
16. Peyton, L.; Gallagher, S.; Hashemzadeh, M.; Triazole antifungals: A review, *Drugs of Today*. **2015**, *51*, 705. <https://doi.org/10.1358/dot.2015.51.12.2421058>.
17. El-Sebaey, S.A.; Recent advances in 1,2,4-Triazole scaffolds as antiviral agents, *ChemistrySelect*. **2020**, *5*, 11654–11680. <https://doi.org/10.1002/slct.202002830>.
18. Shaikh, S.; Nazam, N.; Rizvi, S.M.D.; Ahmad, K.; Baig, M.H.; Lee, E.J.; Choi, I.; Mechanistic Insights into the Antimicrobial Actions of Metallic Nanoparticles and Their Implications for Multidrug Resistance, *International Journal of Molecular Sciences*. **2019**, *20*, 2468. <https://doi.org/10.3390/ijms20102468>.
19. Zhang, Y.; Wu, C.; Zhang, N.; Fan, R.; Ye, Y.; Xu, J.; Recent Advances in the Development of Pyrazole Derivatives as Anticancer Agents. *Int J Mol Sci*. **2023**, *24* (16):12724. doi: 10.3390/ijms241612724.
20. Bhogireddy, D.Nayudu.; Kotala, M. B.; Aduri, R.; Somaiah, N.; Tadiboina, B.R.; Design, synthesis and anticancer assessment of 1,2,3-triazole incorporated 1,3,4-oxadiazole-quinazoline derivatives, *Chemical Data Collections* **2023**, *48*,101073,<https://doi.org/10.1016/j.cdc.2023.101073>.
21. Ahmad, M.K.; Abdollah, N.A.; Shafie, N.H.; Yusof, N.M.; Razak, S.R.A.; Dual-specificity phosphatase 6 (DUSP6): a review of its molecular characteristics and clinical relevance in cancer, *Cancer Biology and Medicine*. **2018**, *15*, 14. <https://doi.org/10.20892/j.issn.2095-3941.2017.0107>.
22. Djemoui, A.; Naouri, A.; Ouahrani, M.R.; Djemoui, D.; Souli, L.; Lahrech, M.; Boukenna, L.; Albuquerque, H.M.T.; Saher, L.; Rocha, D.H.A.; Monteiro, F.L.; Helguero, L.A.; Bachari, K.; Talhi, O.; Silva, A.M.S.; A step-by-step synthesis of triazole-benzimidazole-chalcone hybrids: Anticancer activity in human cells+, *Journal of Molecular Structure*. **2020**, *1204*, 127487. <https://doi.org/10.1016/j.molstruc.2019.127487>.
23. Banerji, A.; Chandrasekhar, K.; Sreenath, K.; Roy, S.; Nag, S.; Saha, K.D.; Synthesis of Triazole-Substituted quinazoline hybrids for anticancer activity and a lead compound as the EGFR blocker and ROS inducer agent, *ACS Omega*. **2018**, *3*, 16134–16142. <https://doi.org/10.1021/acsomega.8b01960>.
24. Perike, N.; Edigi, P.K.; Gurrapu, N.; Thumma, V.; Bujji, S.; Naikal, P.S.; Synthesis, anticancer activity and molecular docking studies of hybrid molecules containing Indole-Thiazolidinedione-Triazole moieties, *ChemistrySelect*. **2022**, *7*, <https://doi.org/10.1002/slct.202203778>.
25. Patil, S.A.; Nesaragi, A.R.; Rodríguez-Berrios, R.R.; Hampton, S.M.; Bugarin, A.; Patil, S.A.; Coumarin Triazoles as Potential Antimicrobial Agents. *Antibiotics (Basel)*. **2023** *12*, 160. doi: 10.3390/antibiotics12010160.

26. Cebeci, Y.U.; Ceylan, S.; Karaoglu, S.A.; Altun, M.; An efficient microwave-assisted synthesis of novel quinolone–triazole and conazole–triazole hybrid derivatives as antimicrobial and anticancer agents. *Journal of Heterocyclic Chemistry* **2023**, *60*, 47–62. <https://doi.org/10.1002/jhet.4560>
27. Becan, L.; Pyra, A.; Rembiałkowska, N.; Bryndal, I. Synthesis, Structural Characterization and Anticancer Activity of New 5-Trifluoromethyl-2-thioxo-thiazolo[4,5-d]pyrimidine Derivatives. *Pharmaceuticals* **2022**, *15*, 92. <https://doi.org/10.3390/ph15010092>.
28. Oyebamiji, A.K.; Semire, B.; In Vitro Biological Estimation of 1,2,3-Triazolo[4,5-d]pyrimidine Derivatives as Anti-breast Cancer Agent: DFT, QSAR and Docking Studies, *Current Pharmaceutical Biotechnology*. **2020**, *21*, 70–78. <https://doi.org/10.2174/1389201020666190904163003>.
29. Kumar, A.; Singh, A.K.; Singh, H.; Vijayan, V.; Kumar, D.; Naik, J.; Thareja, S.; Yadav, J.P.; Pathak, P.; Grishina, M.; Verma, A.; Khalilullah, H.; Jaremko, M.; Emwas, A.H.; Kumar, P.; Nitrogen Containing Heterocycles as Anticancer Agents: A Medicinal Chemistry Perspective. *Pharmaceuticals (Basel)*. **2023**, *16*(2):299. doi: 10.3390/ph16020299.
30. Oyebamiji, A.K.; Tolufashe, G.F.; Oyawoye, O.M.; Oyedepo, T.A.; Semire, B.; Biological Activity of Selected Compounds from *Annona muricata* Seed as Antibreast Cancer Agents: Theoretical Study, *Journal of Chemistry*. **2020**, 1–10. <https://doi.org/10.1155/2020/6735232>.
31. Lü, Y.; Chen, J.; Xiao, M.; Li, W.; Miller, D.D.; An Overview of Tubulin Inhibitors That Interact with the Colchicine Binding Site, *Pharmaceutical Research*. **2012**, *29*, 2943–2971. <https://doi.org/10.1007/s11095-012-0828-z>.
32. Negi, A.S.; Gautam, Y.; Alam, S.; Chanda, D.; Luqman, S.; Sarkar, J.; Konwar, R.; Natural antitubulin agents: Importance of 3,4,5-trimethoxyphenyl fragment, *Bioorganic & Medicinal Chemistry*. **2015**, *23*, 373–389. <https://doi.org/10.1016/j.bmc.2014.12.027>.
33. Romagnoli, R.; Baraldi, P.G.; Prencipe, F.; Oliva, P.; Baraldi, S.; Salvador, M.K.; Cara, C.L.; Bortolozzi, R.; Mattiuzzo, E.; Basso, G.; Viola, G.; Design, synthesis and biological evaluation of 3-substituted-2-oxindole hybrid derivatives as novel anticancer agents, *European Journal of Medicinal Chemistry*. **2017**, *134*, 258–270. <https://doi.org/10.1016/j.ejmech.2017.03.089>.
34. Banimustafa, M.; Kheirollahi, A.; Safavi, M.; Ardestani, S.K.; Aryapour, H.; Foroumadi, A.; Emami, S.; Synthesis and biological evaluation of 3-(trimethoxyphenyl)-2(3H)-thiazole thiones as combretastatin analogs, *European Journal of Medicinal Chemistry*. **2013**, *70*, 692–702. <https://doi.org/10.1016/j.ejmech.2013.10.046>.
35. Ansari, M.; Shokrzadeh, M.; Karima, S.; Rajaei, S.; Hashemi, S.M.; Mirzaei, H.; Fallah, M.; Emami, S.; Design, synthesis and biological evaluation of flexible and rigid analogs of 4H-1,2,4-triazoles bearing 3,4,5-trimethoxyphenyl moiety as new antiproliferative agents, *Bioorganic Chemistry*. **2019**, *93*, 103300. <https://doi.org/10.1016/j.bioorg.2019.103300>.
36. Semire, B.; Odunola, O.A.; Density Functional Theory (DFT) Study on  $\alpha,\alpha$ -Bis(2-benzothiophen-1-yl)-4H-cyclopenta[2,1-b,3;4-b']dithiophene Derivatives for Optoelectronic Devices, *The Journal of Pure and Applied Chemistry Research*. **2019**, *8*, 126–139. <https://doi.org/10.21776/ub.jpacr.2019.008.02.438>.
37. Abdullahi, M.; Adeniji, S.E.; In-silico molecular docking and ADME/Pharmacokinetic prediction studies of some novel carboxamide derivatives as anti-tubercular agents, *Chemistry Africa*. **2020**, *3*, 989–1000. <https://doi.org/10.1007/s42250-020-00162-3>.
38. Afolabi, S.O.; Semire, B.; Akiode, O.K.; Idowu, M.A.; Quantum study on the optoelectronic properties and chemical reactivity of phenoxazine-based organic photosensitizer for solar cell purposes, *Theoretical Chemistry Accounts*. **2022**, *141*, <https://doi.org/10.1007/s00214-022-02882-w>.
39. Ibrahim, A.O.; Semire, B.; Adepoju, A.J.; Latona, D.F.; Oyebamiji, A.K.; Owonikoko, A.D.; Oladuji T.E.; Odunola. O.A.; In Silico investigations on structure, reactivity indices, NLO properties, and bio-evaluation of 1-benzyl-2-phenyl-1H-benzimidazole derivatives using DFT and molecular docking approaches. *Biointer Res Appl Chem*. **2023**, *13*, 233. <https://doi.org/10.33263/BRIAC133.233>
40. Eswaramoorthy, R.; Hailekiros, H.; Sabir, F.K.; Endale, M.; In silico Molecular Docking, DFT Analysis and ADMET Studies of Carbazole Alkaloid and Coumarins from Roots of *Clausena*

- anisata: A Potent Inhibitor for Quorum Sensing, *Advances and Applications in Bioinformatics and Chemistry*. **2021**, 14, 13–24. <https://doi.org/10.2147/aabc.s290912>.
41. Khaldan, A.; Bouamrane, S.; El Mchichi, R. E. M. L.; Maghat, H.; Lakhliifi, M. B. T.; Sbai, A.; In search of new potent  $\alpha$ -glucosidase inhibitors: molecular docking and ADMET prediction. *Moroccan Journal of Chemistry*, **2022**, 10(4), 10-14. <https://doi.org/10.33263/BRIAC134.302>
  42. Rivera-Delgado, E.; Xin, A.W.; Von Recum, H.A.; Using QSARs for predictions in drug delivery, *bioRxiv* (Cold Spring Harbor Laboratory). **2019**, <https://doi.org/10.1101/727172>.
  43. Mahmud, A.W.; Shallangwa, G.A.; Uzairu, A.; QSAR and molecular docking studies of 1,3-dioxoisindoline-4-aminoquinolines as potent antiplasmodium hybrid compounds, *Heliyon*. **2020**, 6, e03449. <https://doi.org/10.1016/j.heliyon.2020.e03449>.
  44. Islam, M.R.; Mahadzir, M.; Modelling and Optimizing of Joint's Fracture Toughness between A7075-T651 and AZ31B Dissimilar Alloys Welded by GMA Spot Welding Method, *Applied Mechanics and Materials*. **2014**, 663, 281–286. <https://doi.org/10.4028/www.scientific.net/amm.663.281>.
  45. Oyebamiji, A.K.; Semire, B.; Dft-Qsar model and docking studies of antiliver cancer (Hepg-2) activities of 1, 4-dihydropyridine based derivatives. *Cancer Biology* **2016**, 6, 69-78. <https://doi.org/10.7537/marscbj06021610>.
  46. Abdullah, S.; Napi, N.N.L.M.; Ahmed, A.N.; Mansor, W.N.W.; Mansor, A.A.; Ismail, M.; Abdullah, A.M.; Ramly, Z.T.A.; Development of Multiple Linear Regression for Particulate Matter (PM10) Forecasting during Episodic Transboundary Haze Event in Malaysia, *Atmosphere*. **2020**, 11, 289. <https://doi.org/10.3390/atmos11030289>.
  47. Vázquez-Jiménez, L.K.; Juárez-Saldívar, A.; Gómez-Escobedo, R.; Delgado-Maldonado, T.; Méndez-Álvarez, D.; Palos, I.; Bandyopadhyay, D.; Gaona-López, C.; Ortiz-Pérez, E.; Noguera-Torres, B.; Ramírez-Moreno, E.; Rivera, G.; Ligand-Based virtual screening and molecular docking of benzimidazoles as potential inhibitors of triosephosphate isomerase identified new trypanocidal agents, *International Journal of Molecular Sciences*. **2022**, 23, 10047. <https://doi.org/10.3390/ijms231710047>.
  48. Purwanto, B.T.; Hardjono, S.; Widiandani, T.; Nasyanka, A.L.; Siswanto, I.; In Silico Study and ADMET prediction of N-(4-fluorophenylcarbamothioyl) Benzamide Derivatives as Cytotoxic Agents. **2021**, 2, 48. <http://www.jonuns.com/index.php/journal/article/view/515>.
  49. Oyebamiji, A.K.; Akintelu, S.A.; Amao, O.P.; Kaka, M.O.; Morakinyo, A.; Amao, F.A.; Semire, B.; Dataset on theoretical bio-evaluation of 1,2,4-thiadiazole-1,2,4-triazole analogues against epidermal growth factor receptor kinase down regulating human lung cancer, *Data in Brief*. **2021**, 37, 107234. <https://doi.org/10.1016/j.dib.2021.107234>.
  50. Nehra, N.; Tital, R.K.; Ghule, V.D.; 1,2,3-Triazoles of 8-Hydroxyquinoline and HBT: synthesis and studies (DNA binding, antimicrobial, molecular docking, ADME, and DFT), *ACS Omega*. **2021**, 6, 27089–27100. <https://doi.org/10.1021/acsomega.1c03668>.
  51. Pal, R.; Chattaraj, P.K.; Electrophilicity index revisited, *Journal of Computational Chemistry*. **2022**, 44, 278–297. <https://doi.org/10.1002/jcc.26886>.
  52. Miar, M.; Shiroudi, A.; Pourshamsian, K.; Oliaey, A.R.; Hatamjafari, F.; Theoretical investigations on the HOMO–LUMO gap and global reactivity descriptor studies, natural bond orbital, and nucleus-independent chemical shifts analyses of 3-phenylbenzo[d]thiazole-2(3H)-imine and its para-substituted derivatives: Solvent and substituent effects, *Journal of Chemical Research*. **2020**, 45, 147–158. <https://doi.org/10.1177/1747519820932091>.
  53. Haribabu, J.; Garisetti, V.; Malekshah, R.E.; Swaminathan, S.; Gayathri, D.; Bhuvanesh, N.; Mangalaraja, R.V.; Echeverría, C.; Karvembu, R.; Design and synthesis of heterocyclic azole based bioactive compounds: Molecular structures, quantum simulation, and mechanistic studies through docking as multi-target inhibitors of SARS-CoV-2 and cytotoxicity, *Journal of Molecular Structure*. **2022**, 1250, 131782. <https://doi.org/10.1016/j.molstruc.2021.131782>.
  54. El-ghamry, M.A.; Elzawawi, F.M.; Aziz, A.A.A.; Nassir, K.M.; Abu-El-Wafa, S.M.; New Schiff base ligand and its novel Cr(III), Mn(II), Co(II), Ni(II), Cu(II), Zn(II) complexes: spectral

- investigation, biological applications, and semiconducting properties, *Scientific Reports*. **2022**, 12, <https://doi.org/10.1038/s41598-022-22713-z>.
55. Ameji, J.P.; Uzairu, A.; Shallangwa, G.A.; Shallangwa, G.A.; Design, pharmacokinetic profiling, and assessment of kinetic and thermodynamic stability of novel anti-Salmonella typhi imidazole analogues, *Bulletin of the National Research Centre*. **2023**, 47, <https://doi.org/10.1186/s42269-023-00983-5>.
  56. Meanwell, N.A.; Lolli, M.L.; Applications of Heterocycles in the Design of Drugs and Agricultural Products, 1st ed., Elsevier, Inc, **2021**. <https://shop.elsevier.com/books/applications-of-heterocycles-in-the-design-of-drugs-and-agricultural-products/meanwell/978-0-12-820181-7>.
  57. Driouche, Y.; Messadi, D.; Quantitative structure-retention relationship model for predicting retention indices of constituents of essential oils of *Thymus vulgaris* (Lamiaceae), *Journal of the Serbian Chemical Society*. **2019**, 84, 405–416. <https://doi.org/10.2298/jsc180817010d>.

**Conflict of interest:** The authors declare no conflict of interest.

*Received 07.05.2025*

*Accepted 24.06.2025*

А. О. Сандей\*, Ш. Абдуллахі\*, О. К. Габріель\*, О. Мозес\*, С. Банджо†. Дослідження in silico похідних триазол-триметоксифенілу як антипроліферативних засобів проти аденокарциномних альвеолярних базальних епітеліальних клітин людини (A549): DFT, QSAR та підходи молекулярного докінгу.

\*Кафедра хімії, Федеральний університет Локоджа, штат Когі, Нігерія

†Лабораторія обчислювальної хімії, кафедра чистої та прикладної хімії, Ладоке Акінтала, Технологічний університет, Р.М.В. 4000, Огбомосо, штат Ойо, Нігерія.

Двадцять вісім наборів синтезованих похідних триазолтриметоксифенілу (TPD) були розглянуті як антипроліферативні препарати проти ліній ракових клітин альвеолярного базального епітелію людини (A549) за допомогою методів DFT, QSAR, профілю ADMET та молекулярного докінгу. Розглянуті сполуки були використані для розробки надійної моделі QSAR, яка була застосована для розробки нових сполук TPD, що могли б служити кандидатами на антипроліферативні препарати проти раку альвеолярного базального епітелію людини (A549). Параметри, отримані з розрахунків DFT, такі як HOMO, LUMO, дипольний момент, хімічна твердість та м'якість, свідчили про перевагу TPD-11 та TPD-25 над етопоксидом як сильних інгібіторів проти ракових клітин альвеолярного базального епітелію людини (A549), що узгоджується з експериментальними даними. Моделювання та валідація QSAR показали значний вплив автокореляції Морана - лаг 4/зважений за поляризованістю (MATS4p), автокореляції центрованого Брото-Моро - лаг 7/зважений за зарядами (ATSC7c), дескрипторів мінімального Е-стану міцності для потенційних водневих зв'язків довжиною 3 (minHBint3) та дескрипторів кількості Е-станів атомного типу: С (naasC) на зареєстровану протиракову активність препаратів у QSAR A549-MLR-GFA ( $R^2 = 0,8146$ , скоригований  $R^2 = 0,7874$ ,  $Q^2_{\text{Loo}} = 0,6015$  та  $R^2 - Q^2_{\text{Loo}} = 0,2582$ ). Використовуючи дані моделі, було запропоновано чотири нові TPD (NTPD-3, NTPD-4, NTPD-6 та NTPD-9). DFT та молекулярний докінговий аналіз показали, що ці чотири сполуки можуть бути кращими інгібіторами проти A549, ніж етопоксид. Однак, властивості ADMET (абсорбція, розподіл, метаболізм, екскреція та токсичність) показали, що NTPD-6 має чудові фармакокінетичні та токсикологічні профілі та може слугувати дороговказом для нових та ефективніших протипухлинних засобів.

**Ключові слова:** триазол-триметоксифеніл, протипухлинні засоби, DFT, QSAR, молекулярний докінг.

**Конфлікт інтересів:** автори повідомляють про відсутність конфлікту інтересів.

*Надіслано до редакції 07.05.2025*

*Прийнято до друку 24.06.2025*

Kharkiv University Bulletin. Chemical Series. Issue 44 (67), 2025